

Soft gluon resummation for heavy quark and dijet cross sections

Nikolaos Kidonakis*

*Department of Physics and Astronomy, University of Edinburgh, Edinburgh EH9 3JZ, Scotland,
United Kingdom*

ABSTRACT: We discuss the resummation of threshold logarithms for heavy quark and dijet cross sections in hadronic collisions. The resummed cross sections are presented at next-to-leading logarithmic accuracy in terms of anomalous dimension matrices which describe the factorization of soft gluons from the hard scattering. We apply our formalism to the calculation of the top quark production cross section at the Fermilab Tevatron.

1. Introduction

Threshold resummations have recently been studied for a variety of hadronic processes, in particular heavy quark and jet production (for a review see Ref. [1]). Near threshold for the production of the final state in these processes one finds large logarithmic corrections which originate from soft gluon emission off the partons in the hard scattering. These logarithms can be resummed to all orders in perturbative QCD. The resummation of the leading threshold logarithms in heavy quark and dijet production cross sections follows the earlier study of the Drell-Yan process [2, 3] since these logarithms originate from the incoming partons and are thus universal.

The resummation of next-to-leading logarithms (NLL) for QCD hard scattering and heavy quark production, in particular, was presented in Refs. [4, 5]. At NLL accuracy one has to take into account the color exchange in the hard scattering. The resummation is formulated in terms of soft anomalous dimension matrices which describe the factorization of soft gluons from the hard scattering. Applications to top and bottom quark production at a fixed center-of-mass scattering angle, $\theta = 90^\circ$ (where the relevant anomalous dimension matrices are diagonal), were discussed in Ref. [6]. More recently the total cross

section was calculated for top quark production at the Tevatron [7]. Resummation for single-particle inclusive cross sections has been considered in Ref. [8].

The NLL resummation formalism for the hadroproduction of dijets has been presented in Refs. [9, 10]. Jet production involves additional complications relative to heavy quark production because of the presence of the final-state jets.

2. Resummation for heavy quark production

We begin with the resummation formalism for heavy quark production. First, we write the factorized form of the cross section and identify singular distributions in it near threshold. Then we refactorize the cross section into functions associated with gluons collinear to the incoming quarks, non-collinear soft gluons, and the hard scattering. Resummation follows from the renormalization properties of these functions. The resummed cross section is written in terms of exponentials of anomalous dimension matrices for each partonic subprocess involved.

2.1 Factorized cross section

We study the production of a pair of heavy quarks of momenta p_1, p_2 , in collisions of hadrons h_a and

*Present address: Department of Physics, Florida State University, Tallahassee, FL 32306-4350, USA.

h_b with momenta p_a and p_b ,

$$h_a(p_a) + h_b(p_b) \rightarrow \bar{Q}(p_1) + Q(p_2) + X, \quad (2.1)$$

with total rapidity y and scattering angle θ in the pair center-of-mass frame. The heavy quark production cross section can be written in a factorized form as a convolution of the perturbatively calculable hard scattering $H_{f\bar{f}}$ with parton distributions $\phi_{f_i/h}$, at factorization scale μ , for parton f_i carrying a momentum fraction x_i of hadron h :

$$\frac{d\sigma_{h_a h_b \rightarrow Q\bar{Q}}}{dQ^2 dy d\cos\theta} = \sum_{f\bar{f}} \int \frac{dx_a}{x_a} \frac{dx_b}{x_b} \phi_{f/h_a}(x_a, \mu^2) \times \phi_{\bar{f}/h_b}(x_b, \mu^2) H_{f\bar{f}} \left(\frac{Q^2}{x_a x_b S}, y, \theta, \frac{Q}{\mu} \right), \quad (2.2)$$

where $S = (p_a + p_b)^2$, $Q^2 = (p_1 + p_2)^2$, and we sum over the two main production partonic subprocesses, $q\bar{q} \rightarrow Q\bar{Q}$ and $gg \rightarrow Q\bar{Q}$. We note that the short-distance hard scattering $H_{f\bar{f}}$ is a smooth function only away from the edges of partonic phase space.

By replacing the incoming hadrons by partons in Eq. (2.2), we may write the infrared regularized partonic scattering cross section, after integrating over the total rapidity of the heavy quark pair, as

$$\frac{d\sigma_{f\bar{f} \rightarrow Q\bar{Q}}}{dQ^2 d\cos\theta} = \int_{\tau}^1 dz \int \frac{dx_a}{x_a} \frac{dx_b}{x_b} \phi_{f/f}(x_a, \mu^2, \epsilon) \times \phi_{\bar{f}/\bar{f}}(x_b, \mu^2, \epsilon) \delta \left(z - \frac{Q^2}{x_a x_b S} \right) \times \hat{\sigma}_{f\bar{f} \rightarrow Q\bar{Q}} \left(1 - z, \frac{Q}{\mu}, \theta, \alpha_s(\mu^2) \right), \quad (2.3)$$

where the argument ϵ represents the universal collinear singularities, and we have introduced a simplified hard-scattering function, $\hat{\sigma}_{f\bar{f} \rightarrow Q\bar{Q}}$. The threshold for the partonic subprocess is given in terms of the variable z ,

$$z \equiv \frac{Q^2}{s}, \quad (2.4)$$

with $s = x_a x_b S$ the invariant mass squared of the incoming partons. At partonic threshold, $z_{\max} = 1$, there is just enough partonic energy to produce the observed final state. We also define a variable $\tau \equiv z_{\min} = Q^2/S$. In general, $\hat{\sigma}$ includes “plus” distributions with respect to

$1 - z$, which arise from incomplete cancellations near threshold between diagrams with real gluon emission and with virtual gluon corrections, with singularities at n th order in α_s of the type

$$-\frac{\alpha_s^n}{n!} \left[\frac{\ln^m(1-z)}{1-z} \right]_+, \quad m \leq 2n-1. \quad (2.5)$$

If we take Mellin transforms (moments with respect to the variable τ) of Eq. (2.3), the convolution becomes a simple product of the moments of the parton distributions and the hard scattering function $\hat{\sigma}$:

$$\int_0^1 d\tau \tau^{N-1} \frac{d\sigma_{f\bar{f} \rightarrow Q\bar{Q}}}{dQ^2 d\cos\theta} = \tilde{\phi}_{f/f}(N, \mu^2, \epsilon) \times \tilde{\phi}_{\bar{f}/\bar{f}}(N, \mu^2, \epsilon) \hat{\sigma}_{f\bar{f} \rightarrow Q\bar{Q}}(N, Q/\mu, \theta, \alpha_s(\mu^2)) \quad (2.6)$$

with the moments of the hard-scattering function and the parton distributions defined, respectively, by

$$\begin{aligned} \hat{\sigma}(N) &= \int_0^1 dz z^{N-1} \hat{\sigma}(z), \\ \tilde{\phi}(N) &= \int_0^1 dx x^{N-1} \phi(x). \end{aligned} \quad (2.7)$$

We then factorize the initial-state collinear divergences into the parton distribution functions, expanded to the same order in α_s as the partonic cross section, and thus obtain the perturbative expansion for the infrared-safe hard scattering function, $\hat{\sigma}$.

We note that under moments divergent distributions in $1 - z$ produce powers of $\ln N$:

$$\int_0^1 dz z^{N-1} \left[\frac{\ln^m(1-z)}{1-z} \right]_+ = \frac{(-1)^{m+1}}{m+1} \ln^{m+1} N + \mathcal{O}(\ln^{m-1} N). \quad (2.8)$$

The hard scattering function $\hat{\sigma}$ is sensitive to soft-gluon dynamics through its $1 - z$ dependence (or the N dependence of its moments). We may now refactorize (moments of) the cross section into N -independent hard components H_{IL} , which describe the truly short-distance hard scattering, center-of-mass distributions ψ , associated with gluons collinear to the incoming partons, and a soft gluon function S_{LI} associated with non-collinear soft gluons. Note that the mass of the heavy quarks eliminates final state collinear

singularities in heavy quark production. This factorization is shown in Fig. 1 where $f\bar{f}$ represents a pair of light quarks or gluons that produce a heavy quark pair. Fig. 2 defines the soft gluon function, S_{LI} , which describes the coupling of soft gluons to the partons, represented by eikonal lines, in the hard scattering. I and L are color indices that describe the color structure of the hard scattering. The hard-scattering function takes contributions from the amplitude and its complex conjugate, $H_{IL} = h^*_L h_I$.

Then we write the refactorized cross section as [5]

$$\int_0^1 d\tau \tau^{N-1} \frac{d\sigma_{f\bar{f} \rightarrow Q\bar{Q}}}{dQ^2 d\cos\theta} = \sum_{IL} H_{IL} \left(\frac{Q}{\mu}, \theta, \alpha_s(\mu^2) \right) \times \tilde{S}_{LI} \left(\frac{Q}{N\mu}, \theta, \alpha_s(\mu^2) \right) \times \tilde{\psi}_{f/f} \left(N, \frac{Q}{\mu}, \epsilon \right) \tilde{\psi}_{\bar{f}/\bar{f}} \left(N, \frac{Q}{\mu}, \epsilon \right). \quad (2.9)$$

The center-of-mass distribution functions ψ absorb the universal collinear singularities of the initial-state partons in the refactorized cross section. They differ from the standard light-cone parton distributions ϕ by being defined at fixed energy rather than light-like momentum fraction. The moments of ψ can then be written as products of moments of ϕ and an infrared safe function.

2.2 Resummation

Now, comparing Eqs. (2.6) and (2.9), we see that the moments of the partonic heavy-quark production cross section are given by

$$\tilde{\sigma}_{f\bar{f} \rightarrow Q\bar{Q}}(N) = \left[\frac{\tilde{\psi}_{f/f}(N, Q/\mu, \epsilon)}{\tilde{\phi}_{f/f}(N, \mu^2, \epsilon)} \right]^2 \times \sum_{IL} H_{IL} \left(\frac{Q}{\mu}, \theta, \alpha_s(\mu^2) \right) \tilde{S}_{LI} \left(\frac{Q}{N\mu}, \theta, \alpha_s(\mu^2) \right) \quad (2.10)$$

where $f\bar{f}$ denotes $q\bar{q}$ or gg , and we have used the relations $\psi_{q/q} = \psi_{\bar{q}/\bar{q}}$ and $\phi_{q/q} = \phi_{\bar{q}/\bar{q}}$. We will now discuss the exponentiation of logarithms of N for each factor in the above equation.

The first factor, $(\tilde{\psi}_{f/f}/\tilde{\phi}_{f/f})^2$, in Eq. (2.10) is universal between electroweak and QCD hard

processes, and was computed first for the Drell-Yan cross section [2]. The resummed expression for this factor is

$$\frac{\tilde{\psi}_{f/f}(N, Q/\mu, \epsilon)}{\tilde{\phi}_{f/f}(N, \mu^2, \epsilon)} = R_{(f)} \exp \left[E^{(f)}(N, Q^2) \right] \times \exp \left\{ -2 \int_{\mu}^Q \frac{d\mu'}{\mu'} \left[\gamma_f(\alpha_s(\mu'^2)) - \gamma_{ff}(N, \alpha_s(\mu'^2)) \right] \right\}, \quad (2.11)$$

where γ_f is the anomalous dimension of the field of flavor f , which is independent of N , and γ_{ff} is the anomalous dimension of the color-diagonal splitting function for flavor f . $R_{(f)}(\alpha_s)$ is an N -independent function of the coupling, which can be normalized to unity at zeroth order. The exponent $E^{(f)}$ is given by

$$E^{(f)}(N, Q^2) = - \int_0^1 dz \frac{z^{N-1} - 1}{1 - z} \times \left\{ \int_{(1-z)^2}^{(1-z)^{m_S}} \frac{d\lambda}{\lambda} A^{(f)} [\alpha_s(\lambda Q^2)] + B^{(f)} [\alpha_s((1-z)^{m_S} Q^2)] + \frac{1}{2} \nu^{(f)} [\alpha_s((1-z)^2 Q^2)] \right\}, \quad (2.12)$$

where the parameter m_S and the resummed coefficients $B^{(f)}$ depend on the factorization scheme. In the DIS and $\overline{\text{MS}}$ factorization schemes we have $m_S = 1$ and $m_S = 0$, respectively. The function $A^{(f)}$ is given by

$$A^{(f)}(\alpha_s) = C_f \left(\frac{\alpha_s}{\pi} + \frac{1}{2} K \left(\frac{\alpha_s}{\pi} \right)^2 \right), \quad (2.13)$$

with $C_f = C_F = (N_c^2 - 1)/(2N_c)$ for an incoming quark, and $C_f = C_A = N_c$ for an incoming gluon, with N_c the number of colors, and $K = C_A(67/18 - \pi^2/6) - 5n_f/9$, where n_f is the number of quark flavors. $B^{(f)}$ is given for quarks in the DIS scheme by $B^{(q)}(\alpha_s) = -3C_F\alpha_s/(4\pi)$, while it vanishes in the $\overline{\text{MS}}$ scheme for quarks and gluons. Finally, the lowest-order approximation to the scheme-independent $\nu^{(f)}$ is $\nu^{(f)} = 2C_f\alpha_s/\pi$.

Next, we discuss resummation for the soft function. The soft matrix S_{LI} depends on N through the ratio $Q/(N\mu)$; its N -dependence can then be resummed by renormalization group analysis. The product $H_{IL}S_{LI}$ of the soft function

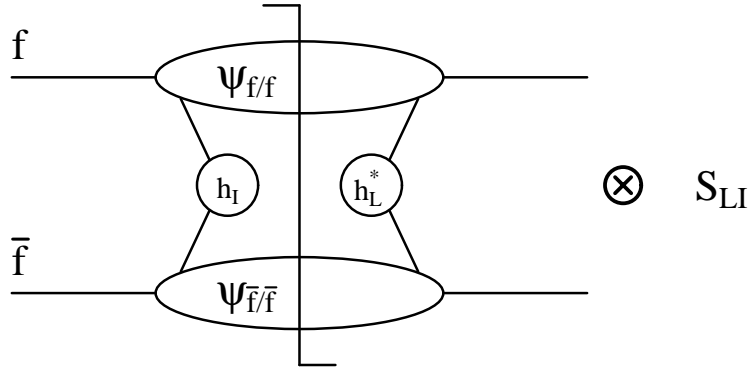


Figure 1: Factorization for heavy quark production near partonic threshold.

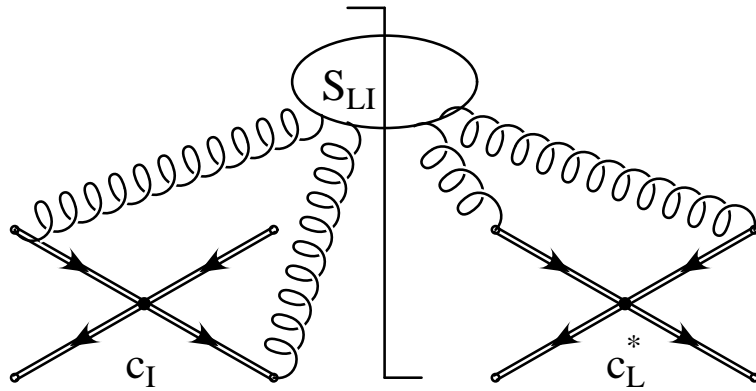


Figure 2: The soft-gluon function S_{LI} in which the vertices c_I, c_L^* link eikonal lines that represent the incoming and outgoing partons.

and the hard factors needs no overall renormalization, because the UV divergences of S_{LI} are balanced by construction by those of H_{IL} . Thus, we have [5]

$$H_{IL}^{(0)} = \prod_{i=f, \bar{f}} Z_i^{-1} (Z_S^{-1})_{IC} H_{CD} \left[\left(Z_S^\dagger \right)^{-1} \right]_{DL},$$

$$S_{LI}^{(0)} = (Z_S^\dagger)_{LB} S_{BA} Z_{S,AI}, \quad (2.14)$$

where $H^{(0)}$ and $S^{(0)}$ denote the unrenormalized quantities, Z_i is the renormalization constant of the i th incoming partonic field external to h_I , and $Z_{S,LI}$ is a matrix of renormalization constants which describes the renormalization of the soft function, including mixing of color structures, and which is defined to include the wave function renormalization for the heavy quarks.

From Eq. (2.14), the soft function S_{LI} satisfies the renormalization group equation

$$\left(\mu \frac{\partial}{\partial \mu} + \beta(g) \frac{\partial}{\partial g} \right) S_{LI} = -(\Gamma_S^\dagger)_{LB} S_{BI}$$

$$-S_{LA}(\Gamma_S)_{AI}, \quad (2.15)$$

where Γ_S is an anomalous dimension matrix that is calculated by explicit renormalization of the soft function. In a minimal subtraction renormalization scheme and with $\epsilon = 4 - n$, where n is the number of space-time dimensions, the matrix of anomalous dimensions at one loop is given by

$$\Gamma_S(g) = -\frac{g}{2} \frac{\partial}{\partial g} \text{Res}_{\epsilon \rightarrow 0} Z_S(g, \epsilon). \quad (2.16)$$

Using Eqs. (2.10), (2.11), and the solution of the renormalization group equation for the soft function, we can write the resummed heavy quark cross section in moment space as

$$\begin{aligned} \tilde{\sigma}_{f\bar{f} \rightarrow Q\bar{Q}}(N) &= R_{(f)}^2 \exp \left\{ 2 \left[E^{(f_i)}(N, Q^2) \right. \right. \\ &\quad \left. \left. - 2 \int_\mu^Q \frac{d\mu'}{\mu'} [\gamma_{f_i}(\alpha_s(\mu'^2)) - \gamma_{f_i f_i}(N, \alpha_s(\mu'^2))] \right] \right\} \\ &\quad \times \text{Tr} \left\{ H \left(\frac{Q}{\mu}, \theta, \alpha_s(\mu^2) \right) \right\} \end{aligned}$$

$$\begin{aligned}
& \times \bar{P} \exp \left[\int_{\mu}^{Q/N} \frac{d\mu'}{\mu'} \Gamma_S^\dagger (\alpha_s(\mu'^2)) \right] \\
& \times \tilde{S} (1, \theta, \alpha_s(Q^2/N^2)) \\
& \times P \exp \left[\int_{\mu}^{Q/N} \frac{d\mu'}{\mu'} \Gamma_S (\alpha_s(\mu'^2)) \right] \Big\} , \quad (2.17)
\end{aligned}$$

where the symbols P and \bar{P} refer to path ordering and the trace is taken in color space.

We may simplify this result by choosing a color basis in which the anomalous dimension matrix Γ_S is diagonal, with eigenvalues λ_I for each basis color tensor labelled by I . Then, we have

$$\begin{aligned}
\tilde{S}_{LI} \left(\frac{Q}{N\mu}, \theta, \alpha_s(\mu^2) \right) &= \tilde{S}_{LI} \left(1, \theta, \alpha_s \left(\frac{Q^2}{N^2} \right) \right) \\
&\times \exp \left[- \int_{Q/N}^{\mu} \frac{d\bar{\mu}}{\bar{\mu}} [\lambda_I(\alpha_s(\bar{\mu}^2)) + \lambda_L^*(\alpha_s(\bar{\mu}^2))] \right] . \quad (2.18)
\end{aligned}$$

Thus, in a diagonal basis, and with $\mu = Q$ and $R_{(f)}$ normalized to unity, we can rewrite the resummed cross section in a simplified form as

$$\begin{aligned}
\tilde{\sigma}_{f\bar{f} \rightarrow Q\bar{Q}}(N) &= H_{IL} (1, \theta, \alpha_s(\mu^2)) \\
&\times \tilde{S}_{LI} (1, \theta, \alpha_s(Q^2/N^2)) \exp \left[E_{LI}^{(f\bar{f})}(N, \theta, Q^2) \right] , \quad (2.19)
\end{aligned}$$

where the exponent is

$$\begin{aligned}
E_{LI}^{(f\bar{f})}(N, \theta, Q^2) &= - \int_0^1 dz \frac{z^{N-1} - 1}{1-z} \\
&\times \left\{ \int_{(1-z)^2}^{(1-z)^{m_S}} \frac{d\lambda}{\lambda} g_1^{(f\bar{f})} [\alpha_s(\lambda Q^2)] \right. \\
&+ g_2^{(f\bar{f})} [\alpha_s((1-z)^{m_S} Q^2)] \\
&\left. + g_3^{(IL, f\bar{f})} [\alpha_s((1-z)^2 Q^2), \theta] \right\} , \quad (2.20)
\end{aligned}$$

with the functions g_1 , g_2 , and g_3 defined by

$$\begin{aligned}
g_1^{(f\bar{f})} &= A^{(f)} + A^{(\bar{f})} , \quad g_2^{(f\bar{f})} = B^{(f)} + B^{(\bar{f})} , \\
g_3^{(IL, f\bar{f})} &= -\lambda_I - \lambda_L^* + \frac{1}{2}\nu^{(f)} + \frac{1}{2}\nu^{(\bar{f})} . \quad (2.21)
\end{aligned}$$

In the next section we present the soft anomalous dimension matrices for heavy quark production through light quark annihilation and gluon fusion; also we give NLO expansions of the resummed cross section in both partonic production channels.

3. Soft anomalous dimension matrices for heavy quark production

3.1 Soft anomalous dimension for $q\bar{q} \rightarrow Q\bar{Q}$

First, we present the soft anomalous dimension matrix for heavy quark production through light quark annihilation,

$$q(p_a, r_a) + \bar{q}(p_b, r_b) \rightarrow \bar{Q}(p_1, r_1) + Q(p_2, r_2) , \quad (3.1)$$

where the p_i 's and r_i 's denote momenta and colors of the partons in the process.

We introduce the Mandelstam invariants

$$\begin{aligned}
s &= (p_a + p_b)^2 , \\
t_1 &= (p_a - p_1)^2 - m^2 , \\
u_1 &= (p_b - p_1)^2 - m^2 , \quad (3.2)
\end{aligned}$$

with m the heavy quark mass, which satisfy $s + t_1 + u_1 = 0$ at partonic threshold.

For the determination of Γ_S we evaluate the one-loop graphs in Figs. 3 and 4. For the $q\bar{q} \rightarrow Q\bar{Q}$ partonic subprocess Γ_S is a 2×2 matrix, since the process can be described by a basis of two color tensors. Here we calculate the soft matrix in the s -channel singlet-octet basis:

$$\begin{aligned}
c_1 &= c_{\text{singlet}} = \delta_{r_a r_b} \delta_{r_1 r_2} , \\
c_2 &= c_{\text{octet}} = (T_F^c)_{r_b r_a} (T_F^c)_{r_2 r_1} , \quad (3.3)
\end{aligned}$$

where the T_F^c are the generators of $SU(3)$ in the fundamental representation. The result of our calculation in a general axial gauge is [1, 4, 5]

$$\Gamma_S = \begin{bmatrix} \Gamma_{11} & \Gamma_{12} \\ \Gamma_{21} & \Gamma_{22} \end{bmatrix} , \quad (3.4)$$

with

$$\begin{aligned}
\Gamma_{11} &= -\frac{\alpha_s}{\pi} C_F [L_\beta + \ln(2\sqrt{\nu_a \nu_b}) + \pi i] , \\
\Gamma_{21} &= \frac{2\alpha_s}{\pi} \ln \left(\frac{u_1}{t_1} \right) , \\
\Gamma_{12} &= \frac{\alpha_s}{\pi} \frac{C_F}{C_A} \ln \left(\frac{u_1}{t_1} \right) , \\
\Gamma_{22} &= \frac{\alpha_s}{\pi} \\
&\times \left\{ C_F \left[4 \ln \left(\frac{u_1}{t_1} \right) - \ln(2\sqrt{\nu_a \nu_b}) - L_\beta - \pi i \right] \right. \\
&\left. + \frac{C_A}{2} \left[-3 \ln \left(\frac{u_1}{t_1} \right) - \ln \left(\frac{m^2 s}{t_1 u_1} \right) + L_\beta + \pi i \right] \right\} , \quad (3.5)
\end{aligned}$$

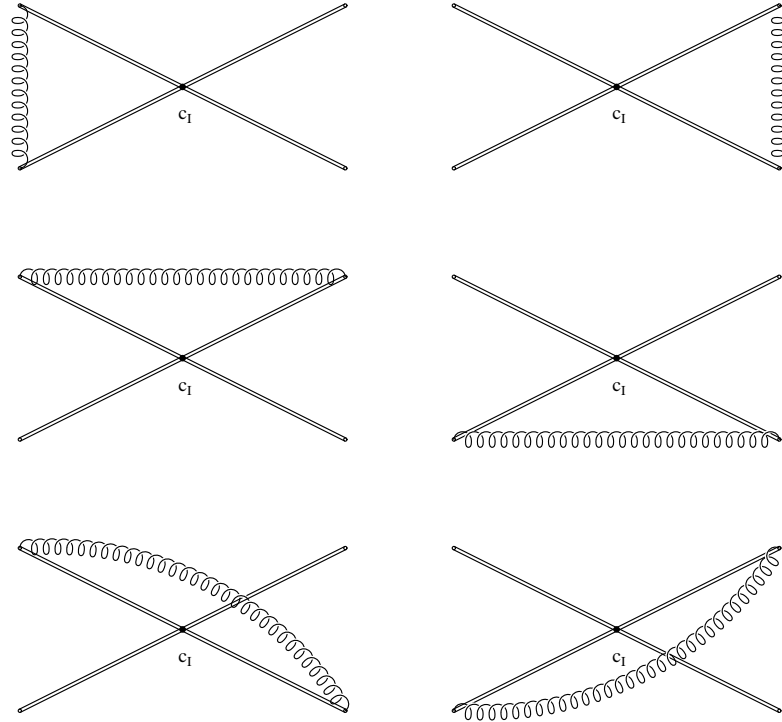


Figure 3: Eikonal vertex corrections to S_{LI} for partonic subprocesses in heavy quark or dijet production.

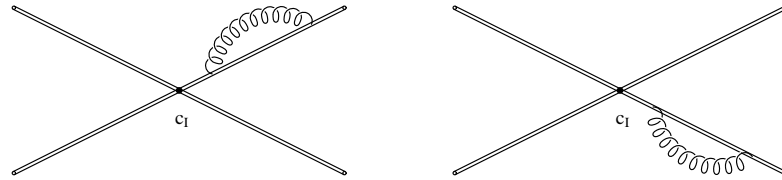


Figure 4: Eikonal self-energy graphs for heavy quark production.

where L_β is the velocity-dependent eikonal function

$$L_\beta = \frac{1 - 2m^2/s}{\beta} \left(\ln \frac{1 - \beta}{1 + \beta} + \pi i \right), \quad (3.6)$$

with $\beta = \sqrt{1 - 4m^2/s}$. The gauge dependence of the incoming eikonal lines is given in terms of $\nu_i \equiv (v_i \cdot n)^2/|n|^2$, with n^μ the gauge vector, which cancels against corresponding terms in the parton distributions. Here the dimensionless velocity vectors v_i^μ are defined by $p_i^\mu = Qv_i^\mu/\sqrt{2}$ and obey $v_i^2 = 0$ for the light incoming quarks and $v_i^2 = 2m^2/Q^2$ for the outgoing heavy quarks. The gauge dependence of the outgoing heavy quarks is cancelled by the inclusion of the self-energy diagrams in Fig. 4.

Γ_S is diagonalized in this singlet-octet color basis at absolute threshold, $\beta = 0$. It is also diag-

onalized for arbitrary β when the parton-parton c.m. scattering angle is $\theta = 90^\circ$ (where $u_1 = t_1$), with eigenvalues that may be read off from Eq. (3.5).

We can expand the resummed heavy quark production cross section to any fixed order in perturbation theory without having to diagonalize the soft anomalous dimension matrix.

The NLO expansion for $q\bar{q} \rightarrow Q\bar{Q}$ in the $\overline{\text{MS}}$ scheme is

$$\begin{aligned} \hat{\sigma}_{q\bar{q} \rightarrow Q\bar{Q}}^{\overline{\text{MS}}(1)}(1 - z, m^2, s, t_1, u_1) &= \sigma_{q\bar{q} \rightarrow Q\bar{Q}}^B \frac{\alpha_s}{\pi} \\ &\times \left\{ 4C_F \left[\frac{\ln(1 - z)}{1 - z} \right]_+ + \left[\frac{1}{1 - z} \right]_+ \right. \\ &\times \left. \left[C_F \left(8 \ln \left(\frac{u_1}{t_1} \right) - 2 - 2 \operatorname{Re} L_\beta + 2 \ln \left(\frac{s}{\mu^2} \right) \right) \right] \right\} \end{aligned}$$

$$+ C_A \left(-3 \ln \left(\frac{u_1}{t_1} \right) + \text{Re } L_\beta - \ln \left(\frac{m^2 s}{t_1 u_1} \right) \right) \right\} , \quad (3.7)$$

where $\sigma_{q\bar{q} \rightarrow Q\bar{Q}}^B$ is the Born cross section. Similar results have been obtained in the DIS scheme. These results are consistent with the approximate one-loop results in Ref. [11]. Analytical and numerical results have also been obtained for the expansions at NNLO [1, 12] in both pair inclusive and single-particle inclusive kinematics.

3.2 Soft anomalous dimension for $gg \rightarrow Q\bar{Q}$

Next, we present the soft anomalous dimension matrix for heavy quark production through gluon fusion,

$$g(p_a, r_a) + g(p_b, r_b) \rightarrow \bar{Q}(p_1, r_1) + Q(p_2, r_2) , \quad (3.8)$$

with momenta and colors labelled by the p_i 's and r_i 's, respectively. Here Γ_S is a 3×3 matrix since the process can be described by a basis of three color tensors. The relevant graphs for the calculation of Γ_S are the same as in Figs. 3 and 4, where now the incoming eikonal lines represent gluons.

We make the following choice for the color basis:

$$\begin{aligned} c_1 &= \delta_{r_a r_b} \delta_{r_2 r_1} , \\ c_2 &= d^{r_a r_b c} (T_F^c)_{r_2 r_1} , \\ c_3 &= i f^{r_a r_b c} (T_F^c)_{r_2 r_1} , \end{aligned} \quad (3.9)$$

where d^{abc} and f^{abc} are the totally symmetric and antisymmetric $SU(3)$ invariant tensors, respectively. Then the anomalous dimension matrix in a general axial gauge is given by [1, 4, 5]

$$\Gamma_S = \begin{bmatrix} \Gamma_{11} & 0 & \frac{\Gamma_{31}}{2} \\ 0 & \Gamma_{22} & \frac{N_c}{4} \Gamma_{31} \\ \Gamma_{31} & \frac{N_c^2 - 4}{4N_c} \Gamma_{31} & \Gamma_{22} \end{bmatrix} , \quad (3.10)$$

where

$$\begin{aligned} \Gamma_{11} &= \frac{\alpha_s}{\pi} [-C_F(L_\beta + 1) \\ &\quad + C_A \left(-\frac{1}{2} \ln(4\nu_a \nu_b) + 1 - \pi i \right)] , \\ \Gamma_{31} &= \frac{\alpha_s}{\pi} \ln \left(\frac{u_1^2}{t_1^2} \right) , \end{aligned}$$

$$\begin{aligned} \Gamma_{22} &= \frac{\alpha_s}{\pi} \left\{ -C_F(L_\beta + 1) + \frac{C_A}{2} \right. \\ &\quad \times \left. \left[-\ln(4\nu_a \nu_b) + 2 + \ln \left(\frac{t_1 u_1}{m^2 s} \right) + L_\beta - \pi i \right] \right\} . \end{aligned} \quad (3.11)$$

We note that Γ_S is diagonalized in this basis at absolute threshold, $\beta = 0$, and also for arbitrary β when the parton-parton c.m. scattering angle is $\theta = 90^\circ$, with eigenvalues that may be read off from Eq. (3.11).

Again, we may expand the resummed cross section for $gg \rightarrow Q\bar{Q}$ at NLO and NNLO or higher. The NLO expansion in the $\overline{\text{MS}}$ scheme is

$$\begin{aligned} \hat{\sigma}_{gg \rightarrow Q\bar{Q}}^{\overline{\text{MS}}(1)}(1-z, m^2, s, t_1, u_1) &= \sigma_{gg \rightarrow Q\bar{Q}}^B \frac{\alpha_s}{\pi} \\ &\times \left\{ 4C_A \left[\frac{\ln(1-z)}{1-z} \right]_+ - 2C_A \ln \left(\frac{\mu^2}{s} \right) \left[\frac{1}{1-z} \right]_+ \right\} \\ &+ \alpha_s^3 K_{gg} B_{QED} \left[\frac{1}{1-z} \right]_+ \left\{ N_c(N_c^2 - 1) \frac{(t_1^2 + u_1^2)}{s^2} \right. \\ &\times \left[\left(-C_F + \frac{C_A}{2} \right) \text{Re } L_\beta + \frac{C_A}{2} \ln \left(\frac{t_1 u_1}{m^2 s} \right) - C_F \right] \\ &+ \frac{N_c^2 - 1}{N_c} (C_F - C_A) \text{Re } L_\beta - (N_c^2 - 1) \ln \left(\frac{t_1 u_1}{m^2 s} \right) \\ &\left. + C_F \frac{N_c^2 - 1}{N_c} + \frac{N_c^2}{2} (N_c^2 - 1) \ln \left(\frac{u_1}{t_1} \right) \frac{(t_1^2 - u_1^2)}{s^2} \right\} \end{aligned} \quad (3.12)$$

where $\sigma_{gg \rightarrow Q\bar{Q}}^B$ is the Born cross section,

$$B_{QED} = \frac{t_1}{u_1} + \frac{u_1}{t_1} + \frac{4m^2 s}{t_1 u_1} \left(1 - \frac{m^2 s}{t_1 u_1} \right) , \quad (3.13)$$

and $K_{gg} = (N^2 - 1)^{-2}$ is a color average factor.

4. Diagonalization and numerical results for $q\bar{q} \rightarrow t\bar{t}$

In this section we give some numerical results for top quark production at the Tevatron.

As we noted in the previous section, the soft anomalous dimension matrices, Γ_S , are in general not diagonal. They are only diagonal at specific kinematical regions, i.e. at absolute threshold, $\beta = 0$, and at a scattering angle $\theta = 90^\circ$. In these cases the exponentiated cross section has a simpler form, Eq. (2.19), and numerical studies are easier to perform. Thus, the resummed cross

section at $\theta = 90^\circ$ for top quark production at the Fermilab Tevatron and bottom quark production at HERA-B were presented in Ref. [6].

In general, however, we must diagonalize Γ_S , i.e. we must find new color bases where Γ_S is diagonal so that the resummed cross section can take the simpler form of Eq. (2.19). The diagonal basis is given by $C' = CR$ where the columns of the matrix R are the eigenvectors of Γ_S . A detailed discussion of the diagonalization procedure has been given in Refs. [1, 7].

The resummed partonic cross section for the process $q\bar{q} \rightarrow Q\bar{Q}$ can be written as [7]

$$\sigma_{q\bar{q}}^{\text{res}}(s, m^2) = \sum_{i,j=1}^2 \int_{-1}^1 d\cos\theta \times \left[- \int_{s_{\text{cut}}}^{s-2ms^{1/2}} ds_4 f_{q\bar{q},ij}(s_4, \theta) \frac{d\bar{\sigma}_{q\bar{q},ij}^{(0)}(s, s_4, \theta)}{ds_4} \right] \quad (4.1)$$

where $s_4 = s + t_1 + u_1$. The $d\bar{\sigma}_{q\bar{q},ij}^{(0)}(s, s_4, \theta)/ds_4$ are color components of the differential of the Born cross section. The function $f_{q\bar{q},ij}$ is given at NLL by the exponential

$$f_{q\bar{q},ij} = \exp[E_{q\bar{q},ij}] = \exp[E_{q\bar{q}} + E_{q\bar{q}}(\lambda_i, \lambda_j)], \quad (4.2)$$

where in the DIS scheme

$$E_{q\bar{q}}^{\text{DIS}} = \int_{\omega_0}^1 \frac{d\omega'}{\omega'} \left\{ \int_{\omega'^2 Q^2/\Lambda^2}^{\omega' Q^2/\Lambda^2} \frac{d\xi}{\xi} \left[\frac{2C_F}{\pi} \left(\alpha_s(\xi) + \frac{1}{2\pi} \alpha_s^2(\xi) K \right) \right] - \frac{3}{2} \frac{C_F}{\pi} \alpha_s \left(\frac{\omega' Q^2}{\Lambda^2} \right) \right\}, \quad (4.3)$$

with $\omega_0 = s_4/(2m^2)$ and Λ the QCD scale parameter. The color-dependent contribution in the exponent is

$$E_{q\bar{q}}(\lambda_i, \lambda_j) = - \int_{\omega_0}^1 \frac{d\omega'}{\omega'} \left\{ \lambda'_i \left[\alpha_s \left(\frac{\omega'^2 Q^2}{\Lambda^2} \right), \theta \right] + \lambda'^*_j \left[\alpha_s \left(\frac{\omega'^2 Q^2}{\Lambda^2} \right), \theta \right] \right\}, \quad (4.4)$$

in both mass factorization schemes, where $i, j = 1, 2$. Here $\lambda' = \lambda - \nu^{(f)}/2$ (see Eq. (2.21)) where the λ 's are the eigenvalues of the soft anomalous dimension matrix. The cutoff s_{cut} in Eq. (4.1) regulates the divergence of α_s at low s_4 : $s_{\text{cut}} > s_{4,\text{min}} = 2m^2\Lambda/Q$. We choose a value of the cutoff consistent with the sum of the first few terms

in the perturbative expansion [6, 13, 14], in the range $30s_{4,\text{min}} < s_{\text{cut}} < 40s_{4,\text{min}}$, which corresponds to a soft gluon energy cutoff of the order of the decay width of the top, thus giving a natural boundary of the nonperturbative region (see also the discussion in [15]). The central value in our cutoff range, $s_{\text{cut}} = 35s_{4,\text{min}}$, corresponds to $s_4/(2m^2) = 0.04$ for $m = 175$ GeV/ c^2 and $\Lambda = 0.2$ GeV.

After the diagonalization of the soft anomalous dimension matrix, the resummed partonic cross section is given at NLL accuracy by [7]

$$\begin{aligned} \sigma_{q\bar{q}}^{\text{res}}(s, m^2) = & - \int_{-1}^1 d\cos\theta \int_{s_{\text{cut}}}^{s-2ms^{1/2}} ds_4 \\ & \times \frac{1}{|\lambda_1 - \lambda_2|^2} \frac{d\bar{\sigma}_{q\bar{q}}^{(0)}(s, s_4, \theta)}{ds_4} \\ & \times \left[\left(\frac{4N_c^2}{N_c^2 - 1} \Gamma_{12}^2 + |\lambda_1 - \Gamma_{11}|^2 \right) e^{E_{q\bar{q},11}} \right. \\ & + \left(\frac{4N_c^2}{N_c^2 - 1} \Gamma_{12}^2 + |\lambda_2 - \Gamma_{11}|^2 \right) e^{E_{q\bar{q},22}} \\ & - \frac{8N_c^2}{N_c^2 - 1} \Gamma_{12}^2 \text{Re} (e^{E_{q\bar{q},12}}) \\ & \left. - 2\text{Re} ((\lambda_1 - \Gamma_{11})(\lambda_2 - \Gamma_{11})^* e^{E_{q\bar{q},12}}) \right]. \quad (4.5) \end{aligned}$$

To calculate the NLL resummed hadronic cross section we convolute the parton distributions $\phi_{i/h}$, for parton i in hadron h , with the partonic cross section:

$$\sigma_{q\bar{q},\text{had}}^{\text{res}}(S, m^2) = \sum_{q=u}^b \int_{\tau_0}^1 d\tau \int_{\tau}^1 \frac{dx}{x} \phi_{q/h_1}(x, \mu^2) \phi_{\bar{q}/h_2} \left(\frac{\tau}{x}, \mu^2 \right) \sigma_{q\bar{q}}^{\text{res}}(\tau S, m^2), \quad (4.6)$$

where $\sigma_{q\bar{q}}^{\text{res}}(\tau S, m^2)$ is defined in Eq. (4.5) and $\tau_0 = (m + \sqrt{m^2 + s_{\text{cut}}})^2/S$.

In Fig. 5 we show numerical results for the $t\bar{t}$ production cross section at the Fermilab Tevatron with $\sqrt{S} = 1.8$ TeV. We use the CTEQ 4D DIS parton densities [16]. The NLO exact cross sections, including the factorization scale dependence, are shown as functions of the top quark mass. We also plot the NLO approximate cross section, i.e. the one-loop expansion of the resummed cross section, calculated with $s_{\text{cut}} = 0$ and $\mu^2 = m^2$. We note the excellent agreement between the NLO exact and approximate cross sections.

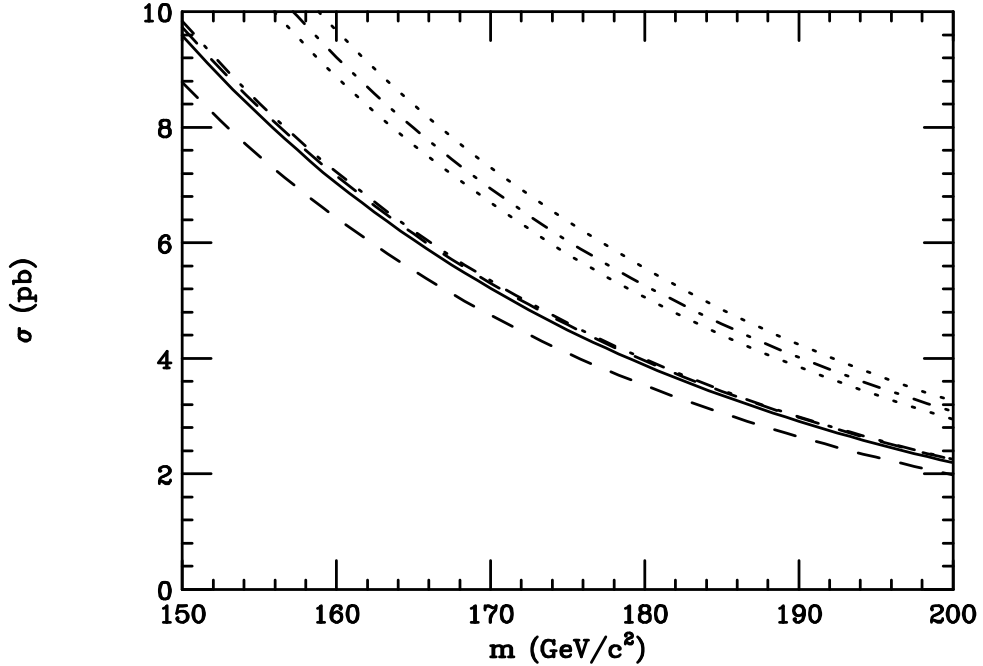


Figure 5: The NLO exact and approximate and the NLL improved hadronic $t\bar{t}$ production cross sections in the $q\bar{q}$ channel and the DIS scheme are given as functions of top quark mass for $p\bar{p}$ collisions at the Tevatron energy, $\sqrt{S} = 1.8$ TeV. The NLO exact cross section is given for $\mu^2 = m^2$ (solid curve), $4m^2$ (lower-dashed) and $m^2/4$ (upper-dashed). The NLO approximate cross section with $s_{\text{cut}} = 0$ is shown for $\mu^2 = m^2$ (lower dot-dashed). The NLL improved cross section, Eq. (4.7), is given for $s_{\text{cut}} = 35s_{4,\text{min}}$ (upper dot-dashed), $30s_{4,\text{min}}$ (upper-dotted) and $40s_{4,\text{min}}$ (lower-dotted).

The scale dependence of the NLL resummed cross section is significantly reduced relative to that of the NLO cross section. In order to match our results to the exact NLO cross section we define the NLL improved cross section

$$\sigma_{q\bar{q},\text{had}}^{\text{imp}} = \sigma_{q\bar{q},\text{had}}^{\text{res}} - \sigma_{q\bar{q},\text{had}}^{\text{NLO,approx}} + \sigma_{q\bar{q},\text{had}}^{\text{NLO,exact}}, \quad (4.7)$$

with the same cut applied to the NLO approximate and the NLL resummed cross sections.

We plot the hadronic improved cross section in Fig. 5 for $\mu^2 = m^2$ along with the variation with s_{cut} . The variation of the improved cross section with change of cutoff is small over the range $30s_{4,\text{min}} < s_{\text{cut}} < 40s_{4,\text{min}}$. At $m = 175$ GeV/ c^2 and $\sqrt{S} = 1.8$ TeV, the value of the improved cross section for $q\bar{q} \rightarrow t\bar{t}$ with $s_{\text{cut}}/(2m^2) = 0.04$ is 6.0 pb compared to a NLO cross section of 4.5 pb at $\mu = m$. The contribution of the $gg \rightarrow Q\bar{Q}$ channel to top quark production at the Tevatron is relatively small. With its inclusion the total $t\bar{t}$ cross section at the Tevatron is

7 pb. Gluon fusion is much more important for b -quark production at HERA-B [14].

5. Resummation for dijet production

Here we review the resummation formalism for the hadronic production of a pair of jets. Dijet production entails additional complications due to the presence of final state jets; otherwise, the formalism is analogous to that for heavy quark production.

5.1 Factorized dijet cross section

We consider dijet production in hadronic processes

$$h_a(p_a) + h_b(p_b) \rightarrow J_1(p_1, \delta_1) + J_2(p_2, \delta_2) + X, \quad (5.1)$$

where δ_1 and δ_2 are the cone angles of the jets. The partonic cross section is infrared safe since the initial-state collinear singularities are factorized into universal parton distribution functions,

and the use of cones removes all the final-state collinear singularities.

We study inclusive dijet cross sections at fixed rapidity interval

$$\Delta y = (1/2) \ln[(p_1^+ p_2^-)/(p_1^- p_2^+)], \quad (5.2)$$

and total rapidity

$$y_{JJ} = (1/2) \ln[(p_1^+ + p_2^+)/(p_1^- + p_2^-)]. \quad (5.3)$$

To construct the dijet cross sections, we define a large invariant, M_{JJ} , which is held fixed. A natural choice is the dijet invariant mass, $M_{JJ}^2 = (p_1 + p_2)^2$, analogous to Q^2 for heavy quark production, but other choices are possible, such as the scalar product of the two jet momenta, $M_{JJ}^2 = 2p_1 \cdot p_2$. We note that for large M_{JJ} at fixed Δy we have a large momentum transfer in the partonic subprocess. The resummed cross section depends critically on the choice for M_{JJ} . We shall see that the leading behavior of the resummed cross section is the same as for heavy quark production when M_{JJ} is the dijet invariant mass, while it is different for the other choice.

The dijet cross section can be written in factorized form as

$$\begin{aligned} \frac{d\sigma_{h_a h_b \rightarrow J_1 J_2}}{dM_{JJ}^2 dy_{JJ} d\Delta y} &= \sum_{f_a, f_b = q, \bar{q}, g} \int \frac{dx_a}{x_a} \frac{dx_b}{x_b} \\ &\times \phi_{f_a/h_a}(x_a, \mu^2) \phi_{f_b/h_b}(x_b, \mu^2) \\ &\times H_{f_a f_b} \left(\frac{M_{JJ}^2}{x_a x_b S}, y, \Delta y, \frac{M_{JJ}}{\mu}, \alpha_s(\mu^2), \delta_1, \delta_2 \right), \end{aligned} \quad (5.4)$$

where H is the hard scattering and the ϕ 's are parton distribution functions.

As for heavy quark production, we may replace the incoming hadrons by partons in the above equation, and integrate over the total rapidity of the jet pair. Then, we can write the infrared regularized partonic cross section, which factorizes as the hadronic cross section, as

$$\begin{aligned} \frac{d\sigma_{f_a f_b \rightarrow J_1 J_2}}{dM_{JJ}^2 d\Delta y} &= \int_{\tau}^1 dz \int \frac{dx_a}{x_a} \frac{dx_b}{x_b} \\ &\times \phi_{f_a/f_a}(x_a, \mu^2, \epsilon) \phi_{f_b/f_b}(x_b, \mu^2, \epsilon) \delta \left(z - \frac{M_{JJ}^2}{s} \right) \\ &\times \sum_f \hat{\sigma}_f \left(1 - z, \frac{M_{JJ}}{\mu}, \Delta y, \alpha_s(\mu^2), \delta_1, \delta_2 \right), \end{aligned} \quad (5.5)$$

where the argument ϵ represents the universal collinear singularities, and we have introduced a simplified hard-scattering function, $\hat{\sigma}_f$, where f denotes the partonic subprocesses. The threshold region is given in terms of the variable z ,

$$z \equiv \frac{M_{JJ}^2}{s}, \quad (5.6)$$

where, as before, $s = x_a x_b S$ with $S = (p_a + p_b)^2$. Partonic threshold is at $z_{\max} = 1$ while the lower limit of z is $z_{\min} \equiv \tau = M_{JJ}^2/S$.

By taking a Mellin transform of the rapidity-integrated partonic cross section, Eq. (5.5), we reduce the convolution to a simple product of moments,

$$\begin{aligned} &\int_0^1 d\tau \tau^{N-1} \frac{d\sigma_{f_a f_b \rightarrow J_1 J_2}}{dM_{JJ}^2 d\Delta y} \\ &= \sum_f \tilde{\phi}_{f_a/f_a}(N, \mu^2, \epsilon) \tilde{\phi}_{f_b/f_b}(N, \mu^2, \epsilon) \\ &\times \tilde{\sigma}_f(N, M_{JJ}/\mu, \alpha_s(\mu^2), \delta_1, \delta_2), \end{aligned} \quad (5.7)$$

with $\tilde{\sigma}_f(N)$ and $\tilde{\phi}(N)$ defined as in Eq. (2.7). We then factorize the initial-state collinear divergences into the light-cone distribution functions $\phi_{f/f}$, expanded to the same order in α_s as the partonic cross section, and thus obtain the perturbative expansion for the infrared-safe hard scattering function, $\tilde{\sigma}_f$.

We can refactorize the cross section, as shown in Fig. 6, into hard components H_{IL} , which describe the truly short-distance hard-scattering, center-of-mass distributions ψ , associated with gluons collinear to the incoming partons, a soft gluon function S_{LI} , associated with non-collinear soft gluons, and jet functions J_i , associated with gluons collinear to the outgoing jets. As for heavy quarks, here I and L denote color indices that describe the color structure of the hard scattering. The refactorized cross section may then be written as

$$\begin{aligned} &\int_0^1 d\tau \tau^{N-1} \frac{d\sigma_{f_a f_b \rightarrow J_1 J_2}}{dM_{JJ}^2 d\Delta y} \\ &= \sum_f \sum_{IL} H_{IL}^{(f)} \left(\frac{M_{JJ}}{\mu}, \Delta y \right) \tilde{S}_{LI}^{(f)} \left(\frac{M_{JJ}}{N\mu}, \Delta y \right) \\ &\times \tilde{\psi}_{f_a/f_a} \left(N, \frac{M_{JJ}}{\mu}, \epsilon \right) \tilde{\psi}_{f_b/f_b} \left(N, \frac{M_{JJ}}{\mu}, \epsilon \right) \\ &\times \tilde{J}_{(f_1)} \left(N, \frac{M_{JJ}}{\mu}, \delta_1 \right) \tilde{J}_{(f_2)} \left(N, \frac{M_{JJ}}{\mu}, \delta_2 \right). \end{aligned}$$

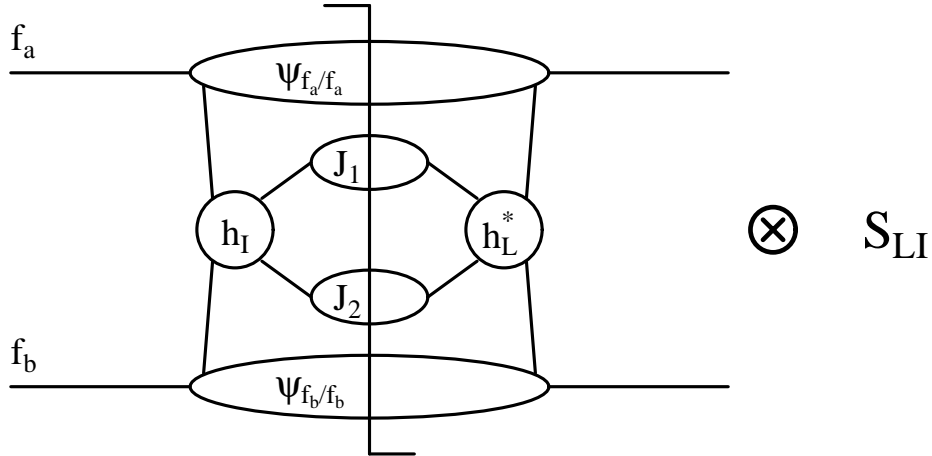


Figure 6: Refactorization for dijet production. The soft gluon function is as in Fig. 2.

. (5.8) with

$$E'_{(f_i)}(N, M_{JJ}) = \int_{\mu}^{M_{JJ}/N} \frac{d\mu'}{\mu'} C'_{(f_i)}(\alpha_s(\mu'^2)), \quad (5.11)$$

where the first term in the series for $C'_{(f_i)}(\alpha_s)$ may be read off from a one-loop calculation. The leading logarithmic behavior of the cross section in this case is not affected by the final state jets, so we always have an enhancement of the cross section at leading logarithm, as is the case for Drell-Yan and heavy quark cross sections.

The moments of the final-state jet with $M_{JJ}^2 = 2p_1 \cdot p_2$ are given by Eq. (5.10) with [9]

$$\begin{aligned} \tilde{\sigma}_f(N) = & \left[\frac{\tilde{\psi}_{f_a/f_a}(N, M_{JJ}/\mu) \tilde{\psi}_{f_b/f_b}(N, M_{JJ}/\mu)}{\tilde{\phi}_{f_a/f_a}(N, \mu^2) \tilde{\phi}_{f_b/f_b}(N, \mu^2)} \right] \\ & \times \sum_{IL} H_{IL}^{(f)} \left(\frac{M_{JJ}}{\mu}, \Delta y \right) \tilde{S}_{LI}^{(f)} \left(\frac{M_{JJ}}{N\mu}, \Delta y \right) \\ & \times \tilde{J}_{(f_1)} \left(N, \frac{M_{JJ}}{\mu}, \delta_1 \right) \tilde{J}_{(f_2)} \left(N, \frac{M_{JJ}}{\mu}, \delta_2 \right). \quad (5.9) \end{aligned}$$

The results for the resummation of the universal ratio ψ/ϕ and the soft gluon function were given in the context of heavy quark production in Section 2. Explicit expressions for the soft anomalous dimension matrices for dijet production will be given in the next section. Thus, the only thing remaining to write down the resummed dijet cross section are expressions for the resummation of the final state jets.

The moments of the final-state jet with $M_{JJ}^2 = (p_1 + p_2)^2$ are given by [9]

$$\tilde{J}_{(f_i)} \left(N, \frac{M_{JJ}}{\mu}, \delta_i \right) = \exp \left[E'_{(f_i)}(N, M_{JJ}) \right], \quad (5.10)$$

where the function $A^{(f)}$ is the same as in Eq. (2.13) and the lowest-order term in $B'_{(f)}$ may be read off from the one-loop jet function. The results include a gauge dependence, which cancels against a corresponding dependence in the soft anomalous dimension matrix. The leading logarithms for final-state jets with $M_{JJ}^2 = 2p_1 \cdot p_2$ are negative and give a suppression to the cross section, in contrast to the initial-state leading-log contributions.

Using Eqs. (5.9), (2.11), and (5.10), together with the evolution of the soft function, we can

write the resummed dijet cross section in moment space as

$$\begin{aligned} \tilde{\sigma}_f(N) = & R_{(f)}^2 \exp \left\{ \sum_{i=a,b} \left[E^{(f_i)}(N, M_{JJ}) \right. \right. \\ & \left. \left. - 2 \int_{\mu}^{M_{JJ}} \frac{d\mu'}{\mu'} [\gamma_{f_i}(\alpha_s(\mu'^2)) - \gamma_{f_i f_i}(N, \alpha_s(\mu'^2))] \right] \right\} \\ & \times \exp \left\{ \sum_{j=1,2} E'_{(f_j)}(N, M_{JJ}) \right\} \\ & \times \text{Tr} \left\{ H^{(f)} \left(\frac{M_{JJ}}{\mu}, \Delta y, \alpha_s(\mu^2) \right) \right. \\ & \times \bar{P} \exp \left[\int_{\mu}^{M_{JJ}/N} \frac{d\mu'}{\mu'} \Gamma_S^{(f)\dagger}(\alpha_s(\mu'^2)) \right] \\ & \times \tilde{S}^{(f)}(1, \Delta y, \alpha_s(M_{JJ}/N^2)) \\ & \left. \times P \exp \left[\int_{\mu}^{M_{JJ}/N} \frac{d\mu'}{\mu'} \Gamma_S^{(f)}(\alpha_s(\mu'^2)) \right] \right\}. \quad (5.13) \end{aligned}$$

This expression is analogous to Eq. (2.17) for heavy quark production except for the addition of the exponents for the final-state jets.

We give explicit expressions for the soft anomalous dimension matrices, Γ_S , for the partonic subprocesses in dijet production in the next section.

6. Soft anomalous dimension matrices for dijet production

We consider partonic subprocesses

$$f_a(p_a, r_a) + f_b(p_b, r_b) \rightarrow f_1(p_1, r_1) + f_2(p_2, r_2), \quad (6.1)$$

where the p_i 's and r_i 's denote momenta and colors of the partons in the process. To facilitate the presentation of the results for Γ_S we use the notation

$$T \equiv \ln \left(\frac{-t}{s} \right) + \pi i, \quad U \equiv \ln \left(\frac{-u}{s} \right) + \pi i, \quad (6.2)$$

where

$$s = (p_a + p_b)^2, \quad t = (p_a - p_1)^2, \quad u = (p_a - p_2)^2, \quad (6.3)$$

are the usual Mandelstam invariants. We note that for the definition of the color basis we can choose any physical channel s , t , or u . We will

use t -channel bases for the partonic processes in dijet production except for the processes $q\bar{q} \rightarrow gg$ and $gg \rightarrow q\bar{q}$ which are better described in terms of s -channel color structures.

Since the full cross section is gauge independent, the gauge dependence in the product of the hard and soft functions, $H^{(f)} S^{(f)}$, must cancel the gauge dependence of the incoming jets, ψ , and outgoing jets, $J_{(f_i)}$. Since the jets are incoherent relative to the hard and soft functions, the gauge dependence of the anomalous dimension matrices $\Gamma_S^{(f)}$ must be proportional to the identity matrix. Then we can rewrite the anomalous dimension matrices as

$$\begin{aligned} (\Gamma_S^{(f)})_{KL} = & (\Gamma_{S'}^{(f)})_{KL} + \delta_{KL} \frac{\alpha_s}{\pi} \\ & \times \sum_{i=a,b,1,2} C_{(f_i)} \frac{1}{2} (-\ln \nu_i - \ln 2 + 1 - \pi i), \quad (6.4) \end{aligned}$$

with $C_{f_i} = C_F$ (C_A) for a quark (gluon), and with $\nu_i \equiv (v_i \cdot n)^2 / |n|^2$. Here the dimensionless and lightlike velocity vectors v_i^μ are defined by $p_i^\mu = M_{JJ} v_i^\mu / \sqrt{2}$ and satisfy $v_i^2 = 0$.

In the following subsections we will present the explicit expressions for $\Gamma_{S'}^{(f)}$ for all the partonic subprocesses in dijet production, by evaluating one-loop diagrams as in Fig. 3. The full anomalous dimension matrices can be retrieved from Eq. (6.4).

6.1 Soft anomalous dimension for $q\bar{q} \rightarrow q\bar{q}$

First, we present the soft anomalous dimension matrix for the process

$$q(p_a, r_a) + \bar{q}(p_b, r_b) \rightarrow q(p_1, r_1) + \bar{q}(p_2, r_2), \quad (6.5)$$

in the t -channel singlet-octet color basis

$$\begin{aligned} c_1 &= \delta_{r_a r_1} \delta_{r_b r_2}, \\ c_2 &= (T_F^c)_{r_1 r_a} (T_F^c)_{r_b r_2}. \end{aligned} \quad (6.6)$$

We find [10, 17]

$$\Gamma_{S'} = \frac{\alpha_s}{\pi} \begin{bmatrix} 2C_F T & -\frac{C_F}{N_c} U \\ -2U & -\frac{1}{N_c}(T - 2U) \end{bmatrix}. \quad (6.7)$$

We note that the dependence on T is diagonal in this t -channel color basis and in the forward region of the partonic scattering, $T \rightarrow -\infty$, where Γ_S becomes diagonal, color singlet exchange is exponentially enhanced relatively to color octet.

6.2 Soft anomalous dimension for $qq \rightarrow qq$ and $\bar{q}\bar{q} \rightarrow \bar{q}\bar{q}$

Next, we consider the process

$$q(p_a, r_a) + q(p_b, r_b) \rightarrow q(p_1, r_1) + q(p_2, r_2) , \quad (6.8)$$

in the t -channel singlet-octet color basis

$$\begin{aligned} c_1 &= (T_F^c)_{r_1 r_a} (T_F^c)_{r_2 r_b} , \\ c_2 &= \delta_{r_a r_1} \delta_{r_b r_2} . \end{aligned} \quad (6.9)$$

The anomalous dimension matrix is [10, 17]

$$\Gamma_{S'} = \frac{\alpha_s}{\pi} \begin{bmatrix} -\frac{1}{N_c}(T+U) + 2C_F U & 2U \\ \frac{C_F}{N_c} U & 2C_F T \end{bmatrix} \quad (6.10)$$

which also applies to the process

$$\bar{q}(p_1, r_1) + \bar{q}(p_2, r_2) \rightarrow \bar{q}(p_a, r_a) + \bar{q}(p_b, r_b) . \quad (6.11)$$

Again, we note that the dependence on T is diagonal in this t -channel color basis, and the color singlet dominates in the forward region of the partonic scattering.

6.3 Soft anomalous dimension for $q\bar{q} \rightarrow gg$ and $gg \rightarrow q\bar{q}$

Here, we present the soft anomalous dimension matrix for the process

$$q(p_a, r_a) + \bar{q}(p_b, r_b) \rightarrow g(p_1, r_1) + g(p_2, r_2) , \quad (6.12)$$

in the s -channel color basis

$$\begin{aligned} c_1 &= \delta_{r_a r_b} \delta_{r_1 r_2} , \\ c_2 &= d^{r_1 r_2 c} (T_F^c)_{r_b r_a} , \\ c_3 &= i f^{r_1 r_2 c} (T_F^c)_{r_b r_a} . \end{aligned} \quad (6.13)$$

We find [10]

$$\begin{aligned} \Gamma_{S'} &= \frac{\alpha_s}{\pi} \quad (6.14) \\ &\times \begin{bmatrix} 0 & 0 & U-T \\ 0 & \frac{C_A}{2}(T+U) & \frac{C_A}{2}(U-T) \\ 2(U-T) & \frac{N_c^2-4}{2N_c}(U-T) & \frac{C_A}{2}(T+U) \end{bmatrix} . \end{aligned}$$

The same anomalous dimension describes also the time-reversed process [4, 5]

$$g(p_1, r_1) + g(p_2, r_2) \rightarrow \bar{q}(p_a, r_a) + q(p_b, r_b) . \quad (6.15)$$

6.4 Soft anomalous dimension for $qg \rightarrow qg$ and $\bar{q}g \rightarrow \bar{q}g$

Next, we consider the “Compton” process

$$q(p_a, r_a) + g(p_b, r_b) \rightarrow q(p_1, r_1) + g(p_2, r_2) , \quad (6.16)$$

in the t -channel color basis

$$\begin{aligned} c_1 &= \delta_{r_a r_1} \delta_{r_b r_2} , \\ c_2 &= d^{r_b r_2 c} (T_F^c)_{r_1 r_a} , \\ c_3 &= i f^{r_b r_2 c} (T_F^c)_{r_1 r_a} . \end{aligned} \quad (6.17)$$

The soft anomalous dimension matrix is [10]

$$\begin{aligned} \Gamma_{S'} &= \frac{\alpha_s}{\pi} \quad (6.18) \\ &\times \begin{bmatrix} (C_F + C_A)T & 0 & U \\ 0 & C_F T + \frac{C_A}{2}U & \frac{C_A}{2}U \\ 2U & \frac{N_c^2-4}{2N_c}U & C_F T + \frac{C_A}{2}U \end{bmatrix} \end{aligned}$$

which also applies to the process

$$\bar{q}(p_1, r_1) + g(p_2, r_2) \rightarrow \bar{q}(p_a, r_a) + g(p_b, r_b) . \quad (6.19)$$

We note that T appears only in the diagonal of the anomalous dimension matrix and that in the forward region ($T \rightarrow -\infty$) the color singlet dominates.

6.5 Soft anomalous dimension for $gg \rightarrow gg$

Finally, we consider the much more complicated process

$$g(p_a, r_a) + g(p_b, r_b) \rightarrow g(p_1, r_1) + g(p_2, r_2) . \quad (6.20)$$

A complete color basis for this process is given by the eight color structures [10]

$$\begin{aligned} c_1 &= \frac{i}{4} [f^{r_a r_b l} d^{r_1 r_2 l} - d^{r_a r_b l} f^{r_1 r_2 l}] , \\ c_2 &= \frac{i}{4} [f^{r_a r_b l} d^{r_1 r_2 l} + d^{r_a r_b l} f^{r_1 r_2 l}] , \\ c_3 &= \frac{i}{4} [f^{r_a r_1 l} d^{r_b r_2 l} + d^{r_a r_1 l} f^{r_b r_2 l}] , \\ c_4 &= P_1(r_a, r_b; r_1, r_2) = \frac{1}{8} \delta_{r_a r_1} \delta_{r_b r_2} , \\ c_5 &= P_{8_S}(r_a, r_b; r_1, r_2) = \frac{3}{5} d^{r_a r_1 c} d^{r_b r_2 c} , \\ c_6 &= P_{8_A}(r_a, r_b; r_1, r_2) = \frac{1}{3} f^{r_a r_1 c} f^{r_b r_2 c} , \\ c_7 &= P_{10+\overline{10}}(r_a, r_b; r_1, r_2) = \frac{1}{2} (\delta_{r_a r_b} \delta_{r_1 r_2}) \end{aligned}$$

$$\begin{aligned}
& - \delta_{r_a r_2} \delta_{r_b r_1}) - \frac{1}{3} f^{r_a r_1 c} f^{r_b r_2 c}, \\
c_8 = P_{27}(r_a, r_b; r_1, r_2) &= \frac{1}{2} (\delta_{r_a r_b} \delta_{r_1 r_2} \\
& + \delta_{r_a r_2} \delta_{r_b r_1}) - \frac{1}{8} \delta_{r_a r_1} \delta_{r_b r_2} - \frac{3}{5} d^{r_a r_1 c} d^{r_b r_2 c}, \\
\end{aligned} \tag{6.21}$$

where the P 's are t -channel projectors of irreducible representations of $SU(3)$ [18], and we use explicitly $N_c = 3$.

The soft anomalous dimension matrix in this basis is [10]

$$\Gamma_{S'} = \begin{bmatrix} \Gamma_{3 \times 3} & 0_{3 \times 5} \\ 0_{5 \times 3} & \Gamma_{5 \times 5} \end{bmatrix}, \tag{6.22}$$

with

$$\Gamma_{3 \times 3} = \frac{\alpha_s}{\pi} \begin{bmatrix} 3T & 0 & 0 \\ 0 & 3U & 0 \\ 0 & 0 & 3(T+U) \end{bmatrix} \tag{6.23}$$

and

$$\begin{aligned}
\Gamma_{5 \times 5} &= \frac{\alpha_s}{\pi} & (6.24) \\
& \times \begin{bmatrix} 6T & 0 & -6U & 0 & 0 \\ 0 & 3T + \frac{3U}{2} & -\frac{3U}{2} & -3U & 0 \\ -\frac{3U}{4} & -\frac{3U}{2} & 3T + \frac{3U}{2} & 0 & -\frac{9U}{4} \\ 0 & -\frac{6U}{5} & 0 & 3U & -\frac{9U}{5} \\ 0 & 0 & -\frac{2U}{3} & -\frac{4U}{3} & -2T + 4U \end{bmatrix}.
\end{aligned}$$

We note that the dependence on T is diagonal and that color singlet exchange dominates in the forward region of the partonic scattering, $T \rightarrow -\infty$, where Γ_S becomes diagonal. This has been the case for all the processes we analyzed in t -channel bases; suppression increases with the dimension of the exchanged color representation.

The calculation of the eigenvalues and eigenvectors of $\Gamma_{S'}$ for the $gg \rightarrow gg$ process is more difficult than for the other partonic processes since we are now dealing with a 8×8 matrix; however, explicit results have been obtained [10]. The eigenvalues of the anomalous dimension matrix, Eq. (6.22), are

$$\begin{aligned}
\lambda_1 &= \lambda_4 = 3 \frac{\alpha_s}{\pi} T, \\
\lambda_2 &= \lambda_5 = 3 \frac{\alpha_s}{\pi} U,
\end{aligned}$$

$$\begin{aligned}
\lambda_3 &= \lambda_6 = 3 \frac{\alpha_s}{\pi} (T+U), \\
\lambda_{7,8} &= 2 \frac{\alpha_s}{\pi} [T+U \\
& \quad \mp 2\sqrt{T^2 - TU + U^2}].
\end{aligned} \tag{6.25}$$

The eigenvectors have the general form

$$\begin{aligned}
e_i &= \begin{bmatrix} e_i^{(3)} \\ 0^{(5)} \end{bmatrix}, \quad i = 1, 2, 3, \\
e_i &= \begin{bmatrix} 0^{(3)} \\ e_i^{(5)} \end{bmatrix}, \quad i = 4 \dots 8,
\end{aligned} \tag{6.26}$$

where the superscripts refer to the dimension. The three-dimensional vectors $e_i^{(3)}$ are given by

$$e_i^{(3)} = \begin{bmatrix} \delta_{i1} \\ \delta_{i2} \\ \delta_{i3} \end{bmatrix}, \quad i = 1, 2, 3. \tag{6.27}$$

The five-dimensional vectors $e_4^{(5)}$, $e_5^{(5)}$ and $e_6^{(5)}$ are given by [10]

$$\begin{aligned}
e_4^{(5)} &= \begin{bmatrix} -15 \\ 6 - \frac{15}{2} \frac{T}{U} \\ -\frac{15}{2} \frac{T}{U} \\ 3 \\ 1 \end{bmatrix}, \quad e_5^{(5)} = \begin{bmatrix} 0 \\ -\frac{3}{2} \\ 0 \\ \frac{3}{4} - \frac{3}{2} \frac{T}{U} \\ 1 \end{bmatrix}, \\
e_6^{(5)} &= \begin{bmatrix} -15 \\ -\frac{3}{2} + \frac{15}{2} \frac{T}{U} \\ \frac{15}{2} - \frac{15}{2} \frac{T}{U} \\ -3 \\ 1 \end{bmatrix}.
\end{aligned} \tag{6.28}$$

The expressions for $e_7^{(5)}$ and $e_8^{(5)}$ are long but can be given succinctly by [10]

$$e_i^{(5)} = \begin{bmatrix} b_1(\lambda'_i) \\ b_2(\lambda'_i) \\ b_3(\lambda'_i) \\ b_4(\lambda'_i) \\ 1 \end{bmatrix}, \quad i = 7, 8, \tag{6.29}$$

where

$$\lambda'_i = \frac{\pi}{\alpha_s} \lambda_i, \tag{6.30}$$

and where the b_i 's are given by

$$\begin{aligned}
 b_1(\lambda'_i) &= \frac{3}{U^2 K'} [80T^4 + 103U^4 - 280UT^3 \\
 &\quad - 300TU^3 + 404T^2U^2 \\
 &\quad + (40T^3 - 16U^3 - 60T^2U + 52TU^2)\lambda'_i], \\
 b_2(\lambda'_i) &= \frac{3}{2K'} [20T^2 - 50UT + 44U^2 \\
 &\quad + (10T - 5U)\lambda'_i], \\
 b_3(\lambda'_i) &= -\frac{3}{2UK'} [40T^3 - 64U^3 - 120T^2U \\
 &\quad + 130TU^2 + (20T^2 + 13U^2 - 20TU)\lambda'_i], \\
 b_4(\lambda'_i) &= \frac{3U}{K'} (2T + 5U - 2\lambda'_i), \tag{6.31}
 \end{aligned}$$

with

$$K' = 20T^2 - 20UT + 21U^2. \tag{6.32}$$

7. Conclusion

We have discussed soft gluon resummation at next-to-leading logarithmic accuracy for heavy quark and dijet production in hadronic collisions. We have constructed the resummed cross sections in terms of exponentials of soft anomalous dimension matrices which describe the factorization of noncollinear soft gluons from the hard scattering. We have presented explicit results for the soft anomalous dimension matrices for the relevant partonic subprocesses. Numerical results have been presented for top quark production at the Fermilab Tevatron. Similar resummations have been recently applied to direct photon [1, 8, 19] and $W +$ jet [1, 20] production, as well as to calculations of transverse momentum and rapidity distributions [12, 21] for heavy quark production.

References

- [1] N. Kidonakis, hep-ph/9902484, submitted to *Int. J. Mod. Phys. A*.
- [2] G. Sterman, *Nucl. Phys.* **B281** (1987) 310.
- [3] S. Catani and L. Trentadue, *Nucl. Phys.* **B327** (1989) 323; **B353** (1991) 183.
- [4] N. Kidonakis, Ph.D. Thesis (SUNY, Stony Brook), UMI-96-36628-mc (microfiche), 1996 [hep-ph/9606474].
- [5] N. Kidonakis and G. Sterman, *Phys. Lett.* **B 387** (1996) 867; *Nucl. Phys.* **B505** (1997) 321 [hep-ph/9705234].
- [6] N. Kidonakis, J. Smith, and R. Vogt, *Phys. Rev.* **D 56** (1997) 1553 [hep-ph/9608343]; N. Kidonakis, in *QCD 97, Nucl. Phys. B (Proc. Suppl.)* **64** (1998) 402 [hep-ph/9708439].
- [7] N. Kidonakis and R. Vogt, *Phys. Rev.* **D 59** (1999) 074014 [hep-ph/9806526].
- [8] E. Laenen, G. Oderda, and G. Sterman, *Phys. Lett.* **B 438** (1998) 173 [hep-ph/9806467].
- [9] N. Kidonakis, G. Oderda, and G. Sterman, *Nucl. Phys.* **B525** (1998) 299 [hep-ph/9801268].
- [10] N. Kidonakis, G. Oderda, and G. Sterman, *Nucl. Phys.* **B531** (1998) 365 [hep-ph/9803241]; in *Proceedings of the 6th International Workshop on Deep Inelastic Scattering and QCD*, ed. Gh. Coremans and R. Roosen (World Scientific, Singapore, 1998), p. 579 [hep-ph/9805279].
- [11] R. Meng, G.A. Schuler, J. Smith, and W.L. van Neerven, *Nucl. Phys.* **B339** (1990) 325.
- [12] N. Kidonakis, E. Laenen, S. Moch, and R. Vogt, in preparation.
- [13] E. Laenen, J. Smith, and W.L. van Neerven, *Nucl. Phys.* **B369** (1992) 543.
- [14] N. Kidonakis and J. Smith, hep-ph/9506253, 1995; *Mod. Phys. Lett.* **A11** (1996) 587 [hep-ph/9606275].
- [15] E.L. Berger and H. Contopanagos, *Phys. Rev.* **D 57** (1998) 253 [hep-ph/9706206].
- [16] H.L. Lai, J. Huston, S. Kuhlmann, F. Olness, J. Owens, D. Soper, W.K. Tung, and H. Weerts, *Phys. Rev.* **D 55** (1997) 1280 [hep-ph/9606399].
- [17] J. Botts and G. Sterman, *Nucl. Phys.* **B325** (1989) 62.
- [18] J. Bartels, *Z. Phys.* **C60** (1993) 471.
- [19] N. Kidonakis and J. Owens, in preparation.
- [20] N. Kidonakis and V. Del Duca, in preparation.
- [21] N. Kidonakis and J. Smith, *Phys. Rev.* **D 51** (1995) 6092 [hep-ph/9502341].